Nano Energy 102 (2022) 107710

Contents lists available at ScienceDirect

Nano Energy

journal homepage: www.elsevier.com/locate/nanoen

Flexible pressure sensor for high-precision measurement of epidermal arterial pulse☆

Xue Wang [a,b], Zhiping Feng [a,b], Yushu Xia [a,b], Gaoqiang Zhang [a,b], Luna Wang [a,b], Liang Chen [a,b], Yufen Wu [c,*], Jin Yang [a,b,**], Zhong Lin Wang [d,*]

[a] Department of Optoelectronic Engineering, Key Laboratory of Optoelectronic Technology and Systems Ministry of Education, Chongqing University, Chongqing 400044, PR China
[b] Department of Optoelectronic Engineering, Chongqing Key Laboratory of Laser Control & Precision Measurement, Chongqing University, Chongqing 400044, PR China
[c] College of Physics and Electronic Engineering, Chongqing Normal University, Chongqing 401331, PR China
[d] Beijing Institute of Nanoenergy and Nanosystems, Chinese Academy of Sciences, Beijing 100083, PR China

ARTICLE INFO

Keywords:
Health monitoring
Epidermal arterial pulse monitoring
Cu powder-coated microstructure

ABSTRACT

The rapid development of flexible pressure sensors (FPSs) has driven pulse-based personalized health monitoring, which is extremely important for the diagnosis and prevention of cardiovascular diseases. However, developing a FPS with a convenient fabrication process to form a natural graded microstructure to capture high-quality physiological signals is still a challenge. In this study, by utilizing polytetrafluoroethylene and Cu powder with a conductive double-sided adhesive, a FPS was developed for high-precision measurement of epidermal arterial pulse based on the principle of triboelectric nanogenerators. By using a convenient coating operation, the Cu powder layer with a 500-nm-scale natural microstructure was formed on the conductive double-sided adhesive. This graded microstructure is composed of Cu powder that enables the FPS to respond sensitively to weak pressure signals, endowing the FPS with a sensitivity of 1.65 V/kPa, response time of 17 ms, and decent stability of up to 4500 cycles. Given its compelling performance, the FPS holds the capability to precisely detect epidermal pulse wave with rich details. The consistency between the pulse waveform at the same position measured by the FPS and a high-precision laser vibrometer (with a displacement resolution of 0.05 pm) is up to 0.9949. Furthermore, the FPS can be applied to acquire pulse wave on different human body parts and monitor arterial pulse changes in real time under different opening and closing behaviors of the arterial vessels. The graded microstructure formed by the Cu powder coating provides a convenient and highly efficient method for mass production of FPSs, which will provide new inspiration for the practical applications of flexible sensors to human health.

1. Introduction

Cardiovascular diseases (CVDs), which cause approximately 17.9 million deaths each year, has become a major factor endangering human health [1]. There are hardly any prior symptoms before the sudden occur of CVDs, but the underlying predisposing conditions long predate the index event [2]. Long-term cardiovascular status monitoring has been reported to be conducive for effective assessment of most CVDs, which is of great significance for the early prevention and diagnosis of CVDs [3]. In clinical medicine, magnetic resonance imaging, digital angiography, Doppler ultrasonography, and electrocardiography are commonly used as routine methods for the diagnosis of CVDs [4]. Although these methods have important applications in clinical diagnosis, challenges in portability, operability, cost of use, and privacy limit their widespread use in active CVD monitoring in everyday life. Of course, portable health monitoring devices are also available, including

☆ Prof Zhong Lin Wang, an author on this paper, is the Editor-in-Chief of Nano Energy, but he had no involvement in the peer review process used to assess this work submitted to Nano Energy. This paper was assessed, and the corresponding peer review managed by Professor Chenguo Hu, also an Associate Editor in Nano Energy.

* Corresponding authors.
** Corresponding author at: Department of Optoelectronic Engineering, Key Laboratory of Optoelectronic Technology and Systems Ministry of Education, Chongqing University, Chongqing 400044, PR China.
E-mail addresses: 20160023@cqnu.edu.cn (Y. Wu), yangjin@cqu.edu.cn (J. Yang), zhong.wang@mse.gatech.edu (Z.L. Wang).

https://doi.org/10.1016/j.nanoen.2022.107710
Received 30 June 2022; Received in revised form 27 July 2022; Accepted 14 August 2022
Available online 17 August 2022
2211-2855/© 2022 Elsevier Ltd. All rights reserved.

pulse oximeters and cuff-based electronic sphygmomanometers, which exhibit remarkable capacities for detecting cardiovascular parameters such as heart rate, oxygen saturation, and blood pressure. However, as people's demand for health-monitoring experiences has been increasing, the flexibility, comfort, and portability of these devices must be optimized.

At present, advances in wearable electronics have driven the rapid development of flexible pressure sensors (FPSs) in physiological signal monitoring [5–9]. Compared with traditional equipment, FPS-based wearable devices hold the advantages of comfort, convenience, miniaturization, and real-time measurement. It can be used as an independent unit to track the health status during the wearer's daily routine. Over the past decade, significant endeavors have been made on FPSs relying on various mechanisms such as ultrasonic [10–12], photoelectric [13–16], piezoelectricity [17–20], piezoresistivity [21–24], and capacitance [25–28]. Especially triboelectricity nanogenerator (TENG) based on triboelectrification and electrostatic induction was proven to be effective for converting mechanical signals of the human body to electrical signals [29–33]. Owing to their characteristics that include a wide selection of materials and being self-powered and universally available, many TENG-based FPSs have been fabricated to monitor joint movements (joint, release), posture (e.g., couch, bow, and blink), and human epidermal physiological signals (e.g., acoustic, respiration, and pulse wave) [34–36]. To enhance the performance of TENG-based FPSs in terms of sensitivity and response frequency band, the introduction of microstructures (hollow, interlock, pyramid, multilevel microstructure, bioinspired structure, etc.) onto the surface of selected materials has been widely used [37–39]. However, the process of fabricating these microstructures often requires complex equipment that can only be operated by professionals, which hinders their optimization process toward low-cost and easy fabrication. Therefore, a simple and cost-effective method to fabricate microstructured FPSs with a capacity to capture high-quality physiological signals must be developed.

In this study, using a Cu powder layer and polytetrafluoroethylene (PTFE) materials, we developed a low-cost triboelectric-based FPS for human epidermal pulse wave monitoring. Relying on the natural graded microstructure surface formed by the Cu powder, the FPS holds a sensitivity of 1.65 V/kPa, response time of 17 ms, and decent stability of up to 4500 cycles. With these capabilities, the FPS was demonstrated to precisely detect epidermal pulse waves with detailed information. The consistency of the measured signal with that measured using a laser vibrometer (with a displacement resolution of 0.05 pm) is up to 0.9949. In addition, the FPS successfully achieved the monitoring of pulse waves on different human body parts and the real-time monitoring of the behaviors of arterial vessels in different open and closed states. Given its characteristics that include cost-effectiveness, a convenient and highly efficient fabrication process, and a capacity for high-precision monitoring of high-quality pulse waves, the FPS holds a promising application prospect in health care.

2. Experimental section

2.1. Testing system for evaluate the performance of the FPS

A function generator (SDG 2122X), an amplifier (PA-1200), and vibration shaker were used for generating a standard excitation signal. High-precision dynamometer (SBT630) to measure the external pressure. The electrometer (Keithley 6514) and data acquisition card (NI BNC 2120) were utilized to capture output signals of the FPS.

2.2. Pulse wave monitoring based on laser vibrometer

The vibrometer head is connected to the vibrometer controller. And the signal processed by the controller is transmitted to the upper computer on the computer through the acquisition card (NI, USB-4432).

2.3. Pulse wave monitoring based on FPS

The FPS is connected to the signal input of the electrometer (Keithley, 6514). And the signal processed by the controller is transmitted to the upper computer on the computer through the acquisition card (NI, USB-4432).

Statement: Participants took part in experiments described herein with informed consent and no formal approval from these experiments was required.

3. Results and discussion

Fig. 1a shows a schematic structure diagram of the FPS, which holds a three-layer configuration. The PTFE (with a thickness of 20 μm) and Cu powder with different capabilities of capturing electrons serve as the two electrification layers. The rough surface formed by the Cu powder is beneficial for improving the performance of the FPS. The optical and scanning electron microscopy images of the Cu powder are shown in Fig. 1b. The conductive double-sided adhesive (CDA) is composed of a conductive non-woven substrate and conductive acrylic acid, exhibiting surface resistance in the *x*-to-*y* direction of 0.2 Ω/sq, which is utilized both as a base material for Cu attachment and to provide a stable and reliable electrode. The remarkable flexibility of the CDA makes it easy to form a ring. The physical photograph and enlarged view of the CDA are shown in Fig. 1c. An as-prepared FPS with a scale of 1.8 × 1.6 cm^2 is illustrated in Fig. 1d. The detailed fabrication procedures of the FPS are presented in Fig. S1.

The Cu powder layer plays an important role in improving the performance of the FPS. In this work, we propose a method to form a Cu powder layer with a natural graded microstructure on the surface of the CDA using a coating process, which is cost-effective and has strong operability. The main fabrication procedures of the Cu layer are illustrated in Fig. 1e. First, the surface of the CDA film was coated with Cu powder. Second, a pressure testing machine was used to apply pressure on the Cu powder to form an intimate contact between the Cu powder and the CDA film. Third, sandpaper was used to scrape off the Cu powder that did not adhere to the CDA. Fourth, the formed Cu layer was placed into the petri dish of the ultrasonic cleaning machine to further remove the Cu powder that does not adhere closely to the surface of the CDA. Finally, a Cu powder layer with a natural graded microstructure was fabricated. Compared with the traditional microstructure fabrication methods, coating is more efficient and suitable for the development of FPSs for industrial mass production. Owing to its good flexibility, the FPS could be naturally attached onto the position of the human artery to capture the epidermal pulse during cardiac ejection. A typical pulse waveform containing three characteristic peaks (advancing, reflected, and dicrotic wave peaks) is shown in Fig. 1f, which can provide valuable information for the diagnosis of cardiovascular diseases such as hypertension and arteriosclerosis. The analog pulse wave signal collected by the FPS can be converted into visual data information through a self-made circuit module, which provides the user with an intuitive sense of their own pulse signal, as shown in Fig. 1g. The circuit module mainly consists of four parts: the low-pass filter is used to filter out useless signals, including useless white noise and powder frequency noise; the amplifier amplifies the signal amplitude for subsequent signal processing; the analog-digital conversion module converts the pulse signal in analog into a digital signal that can be recognized by the microcontroller; and the Bluetooth module sends signals from the hardware to the mobile phone application for processing and displaying of the pulse signal. The entire circuit module has a volume of 2.7 × 2.6 × 0.5 cm^3 (Fig. S2), which allows it to easily form miniaturized wearable devices for monitoring physiological signals.

Fig. 2a shows the operating principle of the FPS, which is the same as that of traditional triboelectric-based pressure sensors. Relying on contact electrification and electrostatic induction, the proximity of the PTFE and Cu powder layer caused by external pressure results in the flow of

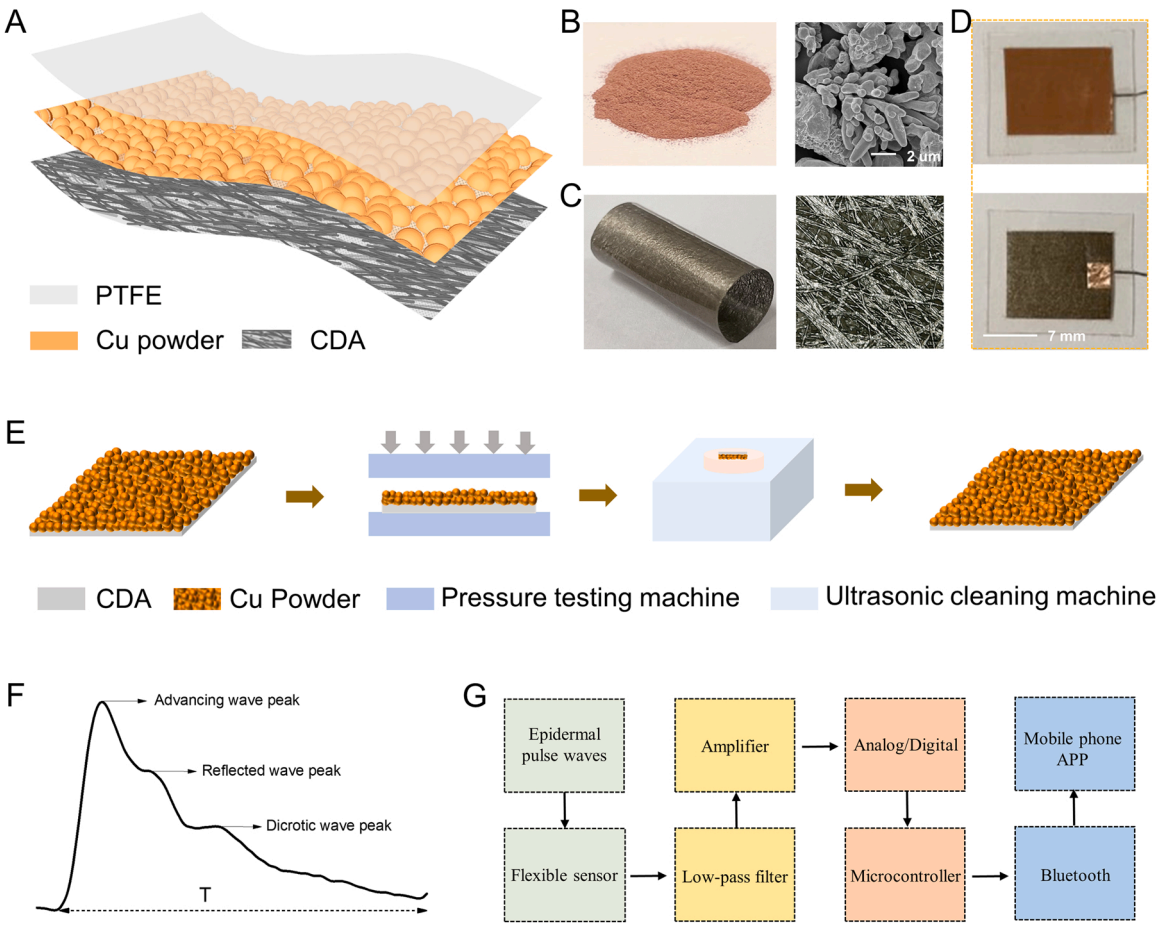

Fig. 1. Construction of the FPS. (a) Schematic structure diagram of the FPS. Optical photographs: (b) the Cu powder, (c) CDA, and (d) the FPS. Scale bar: 7 mm. (e) The main fabrication procedures of the Cu powder layer. (f) A typical pulse waveform containing three characteristic peaks (advancing, reflected, and dicrotic wave peaks). (g) The signal processing flow of the self-made circuit.

electrons from the electrode layer to the reference ground. Reversely, the PTFE tends to return to its original state when the pressure is released, causing electrons to flow from the reference ground to the electrode layer. Thus, a periodic contact-separation process occurs between PTFE and the Cu powder layer under external pressure signals, generating a periodic output voltage. To evaluate the performance of the designed FPS, a testing system was built, as shown in Fig. S3, which mainly consists of three parts: a standard vibration signal generation unit (including a function generator, powder amplifier, and vibration shaker), force acquisition unit (dynamometer and upper PC software), and FPS output voltage acquisition unit (electrometer, data acquisition card, and upper PC software). Detailed information is presented in the Experiment section.

On the basis of the developed testing system, we investigated the output performance of four different sensors with different meshes of Cu powder (Nos. 300, 500, 800, and 1000). For the sensors composed of a single mesh of Cu powder, with the increase in copper powder mesh size, the output voltage of the sensor initially rapidly increased and then decreased (Fig. 2b and Fig. S4). Among the four sensors, the sensor with a No. 800 Cu powder mesh showed the maximum output voltage. The particle diameter of Cu powder decreases with the increase of mesh number, resulting in a larger effective contact-separation area between tribo-pair under small pressure. But the surface formed by Cu powder is close to a flat surface when the mesh size of Cu powder is relatively large, which will easily make the FPS reach saturation state under small pressure. This will make the FPS unable to produce an effective contact-separation process under small dynamic pressure, resulting in a decrease in the output signal. The capability of the FPS to respond to low-frequency signals was characterized by applying pressure signals with different frequencies. As shown in Fig. 2c, the measured results show stable electrical outputs under different frequencies (2, 4, 6, and 8 Hz), which ensure the reliable monitoring of arterial pulsation mainly composed of low-frequency components. Furthermore, the average waveforms of the standard input and output signals over the length of a single period were also obtained through segmentation and normalization, which shows a Pearson correlation coefficient > 0.99 (Fig. 2d).

Pressure sensitivity is an important parameter for evaluating the performance of dynamic pressure sensor, which is defined by the ratio of the change in sensor output voltage to the corresponding pressure range. Fig. 2e depicts the sensitivity of the FPS, which can be divided into two pressure regions. In the < 1.3 kPa low-pressure range, the FPS shows a sensitivity of 1.65 V/kPa. At > 1.3 kPa, the sensitivity of the FPS decreased to 0.17 V/kPa. The output waveform of the FPS under different pressures is shown in Fig. S5. In addition, under the excitation of the square wave signals with a duty ratio of 1%, the FPS shows a response time of 17 ms, as presented in Fig. 2f. In addition, the output voltage exhibited a decent stability in terms of the shape and amplitude of waveform after > 4500 cycles (Fig. 2g), demonstrating the good robustness of the FPS. The output current signals of the FPS under different pressures and frequencies are shown in Fig. S6 and Fig. S7.

Given its compelling performance, the FPS exhibited great application potential in monitoring weak human physiological signals, especially human pulse waves. As can be seen in Fig. 3a, when attached onto the wrist, the FPS is capable of real-time monitoring of the radial pulse waves of a 26-year-old volunteer, presenting tiny blood pressure changes in the arteries of the human body. The enlarged the inset to

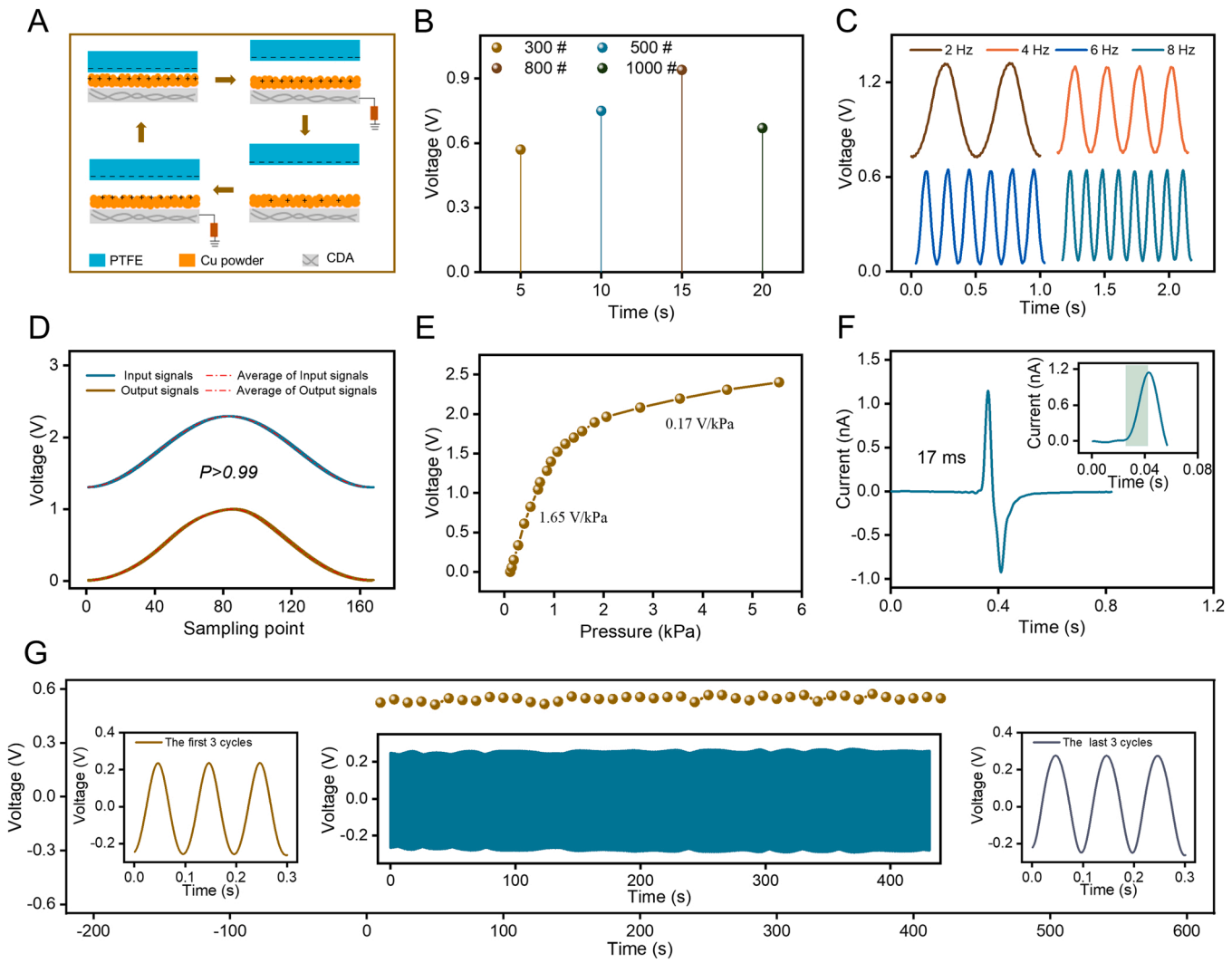

Fig. 2. The output performance of the FPS. (a) The operating principle of the FPS. (b) The output performance of four different sensors with different meshes of Cu powder (Nos. 300, 500, 800, and 1000). (c) The electrical output of the FPS under different frequencies (2, 4, 6, and 8 Hz). (d) The correlation between the input and output signals. (e) The pressure sensitivity of the FPS. (f) Response time characterization of the FPS. (g) The stability of the FPS after > 4500 cycles, and the insets show the first and last three cycles.

clearly show the details of human pulse waves, which holds obvious waveform characteristics and clear three-feature points: advancing (P_1), reflected (P_2), and dicrotic wave peaks (P_3). To study the consistency between the waveforms obtained in the same measurement, the superposition of each period waveform was obtained by segmenting a group of waveforms. As shown in Fig. 3b, the average Pearson correlation coefficient between each cycle was as high as 0.996, and the heart rate value obtained from each cycle waveform basically maintains the same level (62 beats/min).

To demonstrate the accuracy of the FPS for real-time measurement of human arterial pulse, a Polytec's OFV single-point laser vibrometer was utilized to directly measure the displacement of skin tissue caused by a pulse wave. As shown in Fig. 3c and Movie S1, a single-point laser vibrometer head (Polytec, OFV-505) was used as a module for emitting laser and receiving the reflected laser signal, which was connected to a vibrometer controller (Polytec, OFV-5000) that was used as a module for decoding the reflected laser signal into a displacement signal. The detailed acquisition scheme based on the laser and sensor is discussed in the Experiment section. In the measurement, the point with the strongest pulse was determined as the best pulse monitoring position by imitating that in traditional Chinese medicine. Then, the best pulse monitoring point was marked with a marker, and a white square paper was pasted on the point to enhance the reflection of the laser. The height and direction of the laser head were adjusted so that the laser beam is aligned with the marking point and in a vertical position with the marking surface. After the pulse signal was obtained with the laser vibrometer, the radial artery pulse was measured by attaching the FPS to the marked position, with the subject's arm posture unchanged, as shown in Fig. 3d (Movie S2). Similarly, the Pearson correlation coefficients of the signals measured by these two methods in the same measurement were calculated, as shown in Fig. 3e. The inter-group correlation coefficients of the waveforms were measured with these two methods at high levels (the laser-based method is 0.9955 and FPS-based method is 0.9945). The correlation coefficient between the average pulse signal waveforms tested using these two methods was as high as 0.9949, which indicates that the FPS has the ability to accurately collect high-quality pulse signals (Fig. 3f).

Supplementary material related to this article can be found online at doi:10.1016/j.nanoen.2022.107710.

Supplementary material related to this article can be found online at doi:10.1016/j.nanoen.2022.107710.

To evaluate the stability of the FPS for continuous pulse wave monitoring, a 25-year-old subject's radial pulse wave was continuously measured for 90 s, as shown in Fig. 4a. The first and last three cycle

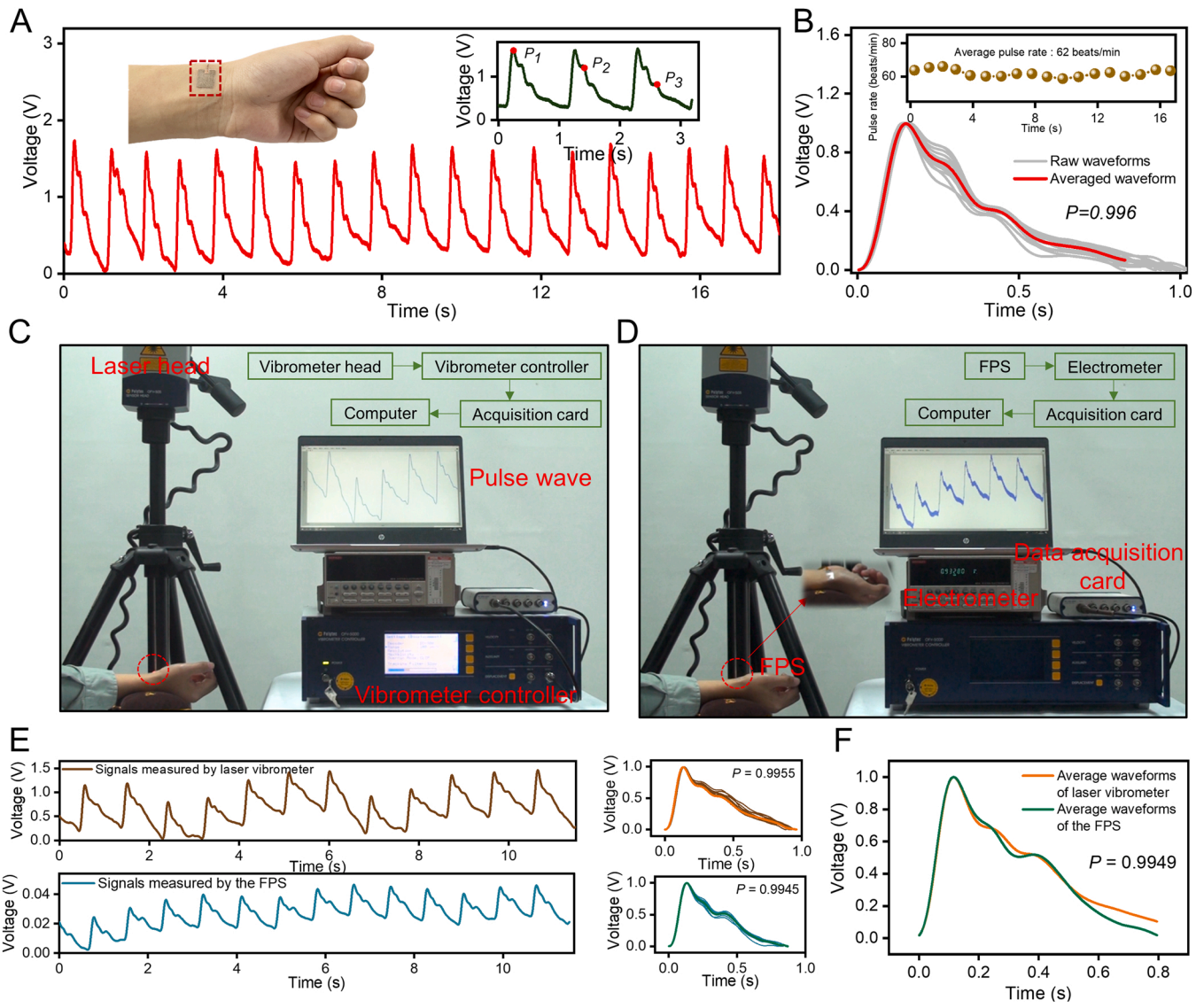

Fig. 3. Arterial pulse wave detected with a laser vibrometer and FPS. (a) The radial pulse wave of a 26-year-old volunteer when the FPS was attached onto the wrist. (b) The consistency of the waveform and the change in heart rate in the same measurement. (c) The arterial pulse wave measured with a laser vibrometer. (d) The arterial pulse wave measured with the FPS. (e) Pearson correlation coefficients of the signals measured using the two methods. (f) The correlation coefficient between the average pulse signal waveform tested with a laser vibrometer and FPS.

waveforms present high similarity in amplitude and shape (Fig. S8). The HR plays a significant role in assessing the risk of cardiac death, which can be characterized by a Poincare plot (Note S1). Fig. 4b exhibits the Poincare plot geometry of the measured signals in Fig. 4a, which holds a standard comet-like shape, with a RR_n ranging from 0.81 to 0.96 s (normal range: 0.6–1 s). SD_1, SD_2, and SD_{12} were also obtained, with values of 15.0, 40.4, and 0.37 ms (normal value < 0.55), respectively. All the obtained data from the Poincare plot indicate a healthy heart state. In addition, we can withdraw some parameters underlying the waveform, such as heart rate (HR), augmentation index (AIr), reflection index (RI), systolic upstroke time (UI), and the time difference between P_1 and P_3 (each parameter calculated as shown in Fig. S9), which provide important values for early prevention and diagnosis of CVDs. The changes in the other parameters extracted from the measured signals are shown in Fig. S10. As is known to all, the pulse wave originates from the heart and travels through blood vessels throughout the whole body [40]. Thus, besides the wrist, many other arterial positions can be used to monitor human arterial pulse. To investigate the FPS's capability of monitoring the pulse of other arteries, it was worn around the neck and ankle. The pulse wave measured at these two positions are respectively shown in Fig. S11. This clearly shows that P_2 is barely represented in the pulse waveform at the ankle, which is the result of the superposition of the advancing and reflected waves [41]. In addition, the FPS proved capable of monitoring pulse signals in different people. The radial pulse was successfully measured in a woman aged 26 years and a man aged 25 years (Fig. 4c and d, Movie S3 and S4), which show clear feature points (P_1, P_2, and P_3).

Supplementary material related to this article can be found online at doi:10.1016/j.nanoen.2022.107710.

In another application, we used the FPS to monitor the behavior of the artery from an open state to a fully closed state and then to again to an open state. The measurement process is shown in Fig. 4e. An inflatable cuff is used to wrap the subject's upper arm to apply pressure to the artery. The Omron sphygmomanometer is used to monitor real-time changes in blood pressure. The FPS is attached to the wrist to continuously monitor radial pulse waves. Before the cuff is inflated, the artery is completely open. Once the blood pressure is measured, the pressure from the cuff causes the artery to gradually close and then open again, as

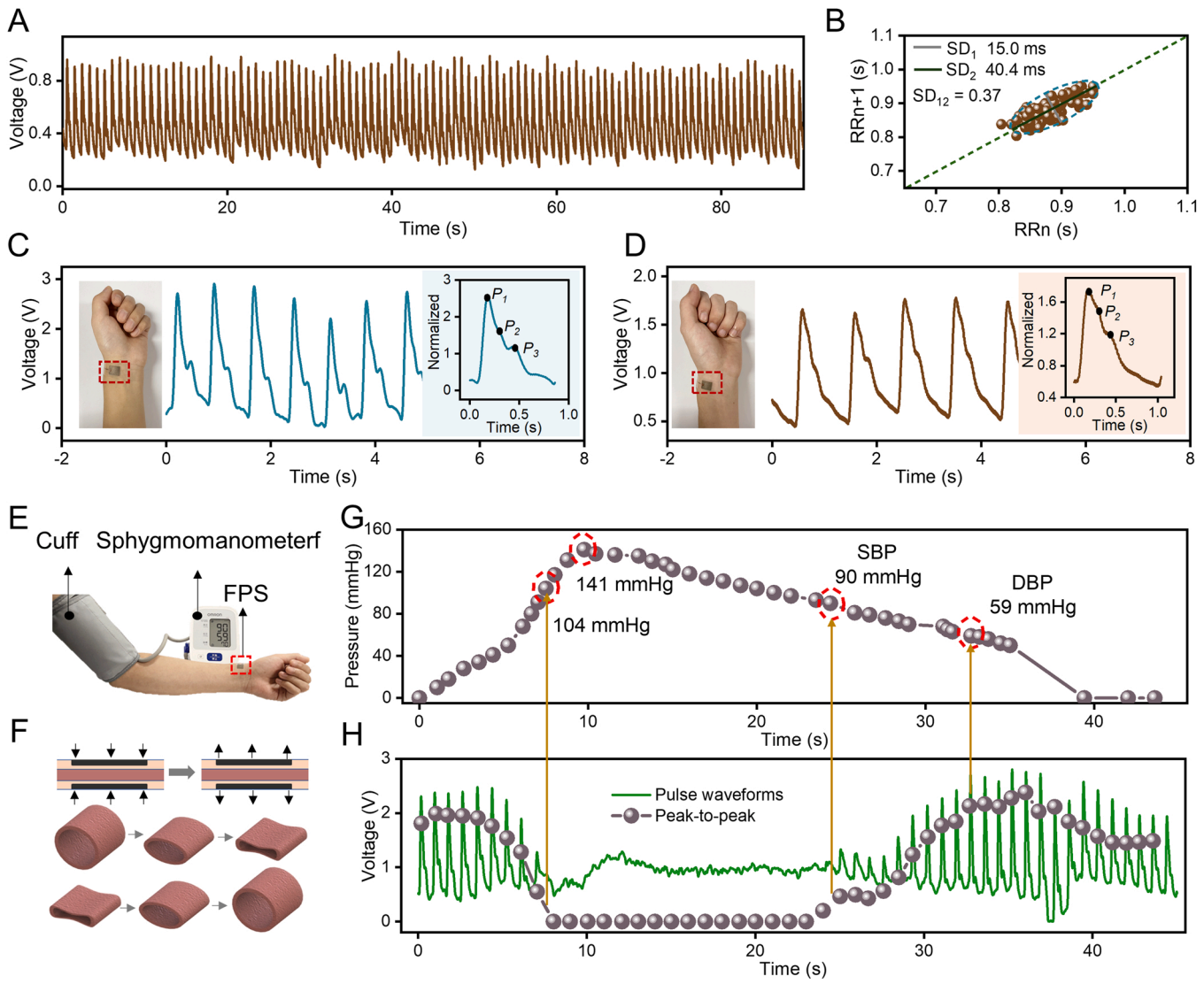

Fig. 4. Arterial pulse wave monitoring under different conditions. (a) Continuous pulse wave monitoring for 90 s (b) The HR characterized by a Poincare plot. (c) The radial pulse wave measured in a woman aged 26 years. (d) The radial pulse wave measured in a man aged 25 years. (e) The Omron sphygmomanometer and FPS are used to measure blood pressure and pulse wave simultaneously. (f) Changes in blood vessels during cuff compression. (g) Changes in cuff pressure during measurement. (h) Changes in pulse wave during measurement.

shown in Fig. 4f. The cuff inflated well above 104 mmHg to occlude arterial flow, without a radial pulse wave. After reaching 141 mmHg, the cuff pressure then slowly deflated to 90 mmHg, at which point, the cuff pressure equals the arterial blood pressure (with the cuff pressure value equal to the systolic blood pressure). At the same time, the radial artery suddenly appeared but did not fully return to normal. As the cuff pressure continued to decrease, the radial pulse amplitude gradually increased. The pulse amplitude did not change drastically until the cuff pressure was 59 mmHg (the cuff pressure value at this point was equal to the diastolic blood pressure). The radial pulse returned to its initial state when the pressure of the cuff was fully released (Fig. 4g and h). This process shows that the FPS can sense the change in arterial pulse in real time. On the other hand, it also reveals the principle of using an electronic sphygmomanometer to measure blood pressure.

Where there is life, there is a pulse, which accompanies the whole life cycle of a person. It is the time variability of the pulse that enables people to discover the regularity between the pulse and physiological changes, thus providing reference information for the early prevention and diagnosis of CVDs. Therefore, we used a FPS to monitor the wrist pulse signals of the same individual at different times on the same day. Pulse waves were collected every 3 h from 7:00 am to 10:00 pm. In Fig. 5a and f, three consecutive cycle pulse waves were displayed at different times (7:00 am, 10:00 am, 1:00 pm, 4:00 pm, 7:00 pm, and 10:00 pm). The correlation coefficients between the mean values of each waveform were calculated, as shown in the table in Fig. 5g. It can be clearly seen that the correlation coefficients of the waveforms at different times were $\geq$ 0.967, and the maximum value was 0.993, which suggests that the pulse shapes of the same individual in a resting state on the same day are not remarkably different. In addition, the corresponding calculated HR, UI, and PPT are shown in Fig. 5h. The participants' HR were significantly higher at 7:00 am and lower in rest of the time, but the change in UI was the opposite to that in HR. The minimum value of the PPT was obtained at 13:00, and remained relatively stable in the rest stages. In different measurements, the pulse wave itself in the same individual will change due to the influence of the individual's own physiological state and human activities. These statistical results show that the proposed FPS can be used for continuous and noninvasive monitoring of arterial pulse, which holds great promise for early prevention and diagnosis of CVDs.

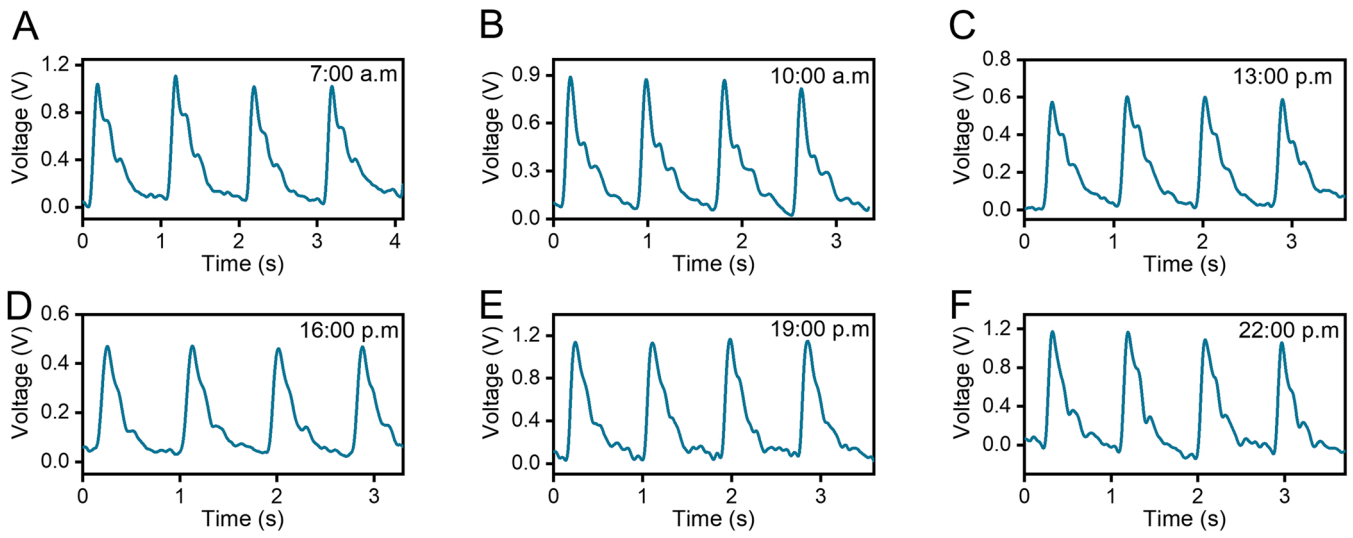

G

Table 1 Pulse consistency at different times

	07:00	10:00	13:00	16:00	19:00	22:00
07:00	1.000	0.980	0.993	0.969	0.976	0.978
10:00	0.980	1.00	0.978	0.976	0.981	0.977
13:00	0.993	0.978	1.000	0.967	0.983	0.986
16:00	0.969	0.976	0.967	1.000	0.990	0.987
19:00	0.976	0.981	0.983	0.990	1.000	0.990
22:00	0.978	0.986	0.986	0.987	0.990	1.000

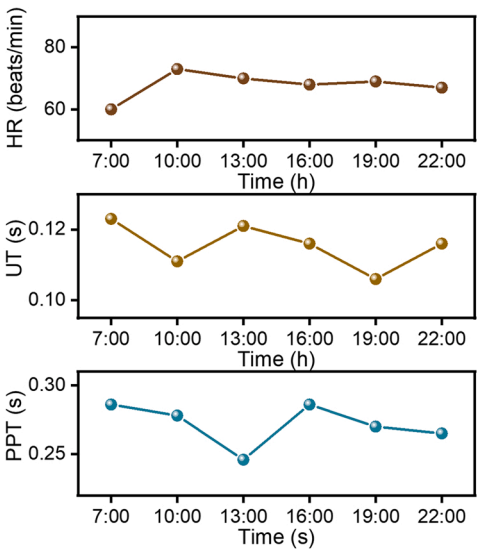

Fig. 5. The pulse signal of the same subject measured at different times. (a–f) The pulse wave was collected every 3 h, from 7:00 am to 10:00 pm. (g) The correlation coefficients between the mean values of each waveform at different times. (h) The changes in HR, UI, and PPT at different times.

4. Conclusions

In this work, a triboelectric-based FPS is proposed for human epidermal pulse wave monitoring. By using a coating method, a Cu powder layer was created to form a natural graded microstructured surface. This provides a low-cost and highly efficient way to fabricate FPS. Featured with a sensitivity of 1.65 V/kPa, response time of 17 ms, and decent stability of up to 4500 cycles, the FPS holds a capability of precisely detecting epidermal pulse waves with detailed information. The measured pulse signals showed obvious characteristic points and maintained a consistency of 0.9949 with those measured using a laser vibrometer. Furthermore, the FPS can be successfully applied to monitor arterial pulse at different positions in different people and to capture real-time changes in the radial artery pulse when the brachial artery is subjected to cuff pressure. Given its characteristics that include its being cost-effective and a convenient fabrication process, and having a capacity for high-quality pulse waves, the FPS has a promising application prospect in health-care.

CRediT authorship contribution statement

The corresponding author is responsible for ensuring that the descriptions are accurate and agreed by all authors. **Xue Wang:** Investigation, Writing – original draft, Methodology, Visualization. **Zhiping Feng:** Investigation, Data curation, Writing – original draft, Visualization. **Yushu Xia:** Investigation, Writing – review & editing. **Gaoqiang Zhang:** Investigation, Data curation, Visualization. **Luna Wang:** Investigation, Visualization. **Liang Chen:** Investigation, Visualization. **Yufen Wu**: Conceptualization, Methodology, Writing – review & editing. **Jin Yang:** Conceptualization, Supervision, Project administration, Funding acquisition. **Zhong Lin Wang:** Conceptualization, Supervision, Writing – review & editing.

Declaration of Competing Interest

The authors declare that they have no known competing financial interests or personal relationships that could have appeared to influence the work reported in this paper.

Data Availability

Data will be made available on request.

Acknowledgments

This work was supported by the National Key Research and Development Project (2021YFA1201602), the Natural Science Foundation of Innovative Research Groups under Grant cstc2020jcyj-cxttX0005, the Natural Science Foundation Projects of Chongqing cstc2022ycjh-bgzxm0206 , and the Fundamental Research Funds for the Central Universities (Nos. 2018CDQYGD0020, cqu2018CDHB1A05).

Appendix A. Supporting information

Supplementary data associated with this article can be found in the online version at doi:10.1016/j.nanoen.2022.107710.

References

[1] G. Chen, C. Au, J. Chen, Textile triboelectric nanogenerators for wearable pulse wave monitoring, Trends Biotechnol. 39 (2021) 1078–1092.
[2] K. Kario, J.A. Chirinos, R.R. Townsend, M.A. Weber, A. Scuteri, A. Avolio, S. Hoshide, T. Kabutoya, H. Tomiyama, K. Node, M. Ohishi, S. Ito, T. Kishi, H. Rakugi, Y. Li, C.H. Chen, J.B. Park, J.G. Wang, Systemic hemodynamic atherothrombotic syndrome (SHATS)-Coupling vascular disease and blood pressure variability: Proposed concept from pulse of Asia, Prog. Cardiovasc. Dis. 63 (2020) 22–32.
[3] Y. Fang, Y. Zou, J. Xu, G. Chen, Y. Zhou, W. Deng, X. Zhao, M. Roustaei, T.K. Hsiai, J. Chen, Ambulatory cardiovascular monitoring via a machine-learning-assisted textile triboelectric sensor, Adv. Mater. 33 (2021), e2104178.
[4] S. Chen, N. Wu, S. Lin, J. Duan, Z. Xu, Y. Pan, H. Zhang, Z. Xu, L. Huang, B. Hu, J. Zhou, Hierarchical elastomer tuned self-powered pressure sensor for wearable multifunctional cardiovascular electronics, Nano Energy 70 (2020), 104460.
[5] Z. Ma, S. Li, H. Wang, W. Cheng, Y. Li, L. Pan, Y. Shi, Advanced electronic skin devices for healthcare applications, J. Mater. Chem. B 7 (2019) 173–197.
[6] H. Wang, J. Cheng, Z. Wang, L. Ji, Z.L. Wang, Triboelectric nanogenerators for human-health care, Sci. Bull. 66 (2021) 490–511.
[7] X. Wang, Z. Liu, T. Zhang, Flexible sensing electronics for wearable/attachable health monitoring, Small 13 (2017), 1602790.
[8] S. Yao, P. Swetha, Y. Zhu, Nanomaterial-enabled wearable sensors for healthcare, Adv. Health Mater. 7 (2018), 1700889.
[9] F. Wang, P. Jin, Y. Feng, J. Fu, P. Wang, X. Liu, Y. Zhang, Y. Ma, Y. Yang, A. Yang, X. Feng, Flexible doppler ultrasound device for the monitoring of blood flow velocity, Sci. Adv. 7 (2021) eabi9283.
[10] J.R. Sempionatto, M. Lin, L. Yin, E. De la Paz, K. Pei, T. Sonsa-Ard, A.N. de Loyola Silva, A.A. Khorshed, F. Zhang, N. Tostado, S. Xu, J. Wang, An epidermal patch for the simultaneous monitoring of haemodynamic and metabolic biomarkers, Nat. Biomed. Eng. 5 (2021) 737–748.
[11] C. Wang, X. Li, H. Hu, L. Zhang, Z. Huang, M. Lin, Z. Zhang, Z. Yin, B. Huang, H. Gong, S. Bhaskaran, Y. Gu, M. Makihata, Y. Guo, Y. Lei, Y. Chen, C. Wang, Y. Li, T. Zhang, Z. Chen, A.P. Pisano, L. Zhang, Q. Zhou, S. Xu, Monitoring of the central blood pressure waveform via a conformal ultrasonic device, Nat. Biomed. Eng. 2 (2018) 687–695.
[12] E.O. Polat, G. Mercier, I. Nikitskiy, E. Puma, T. Galan, S. Gupta, M. Montagut, J. J. Piqueras, M. Bouwens, T. Durduran, G. Konstantatos, S. Goossens, F. Koppens, Flexible graphene photodetectors for wearable fitness monitoring, Sci. Adv. 5 (2019) eaaw7846.
[13] Y. Lee, J.W. Chung, G.H. Lee, H. Kang, J.-Y. Kim, C. Bae, H. Yoo, S. Jeong, H. Cho, S.-G. Kang, J.Y. Jung, D.-W. Lee, S.G. Hahm, Y. Kuzumoto, S.J. Kim, Z. Bao, Y. Hong, Y. Yun, S. Kim, Standalone real-time health monitoring patch based on a stretchable organic optoelectronic system, Sci. Adv. 7 (2021) eabg9180.
[14] H. Jinno, T. Yokota, M. Koizumi, W. Yukita, M. Saito, I. Osaka, K. Fukuda, T. Someya, Self-powered ultraflexible photonic skin for continuous bio-signal detection via air-operation-stable polymer light-emitting diodes, Nat. Commun. 12 (2021) 2234.
[15] J. Kim, P. Gutruf, A.M. Chiarelli, S.Y. Heo, K. Cho, Z. Xie, A. Banks, S. Han, K. I. Jang, J.W. Lee, K.T. Lee, X. Feng, Y. Huang, M. Fabiani, G. Gratton, U. Paik, J. A. Rogers, Miniaturized battery-free wireless systems for wearable pulse oximetry, Adv. Funct. Mater. 27 (2017), 1604373.
[16] J. Park, M. Kim, Y. Lee, H.S. Lee, H. Ko, Fingertip skin–inspired microstructured ferroelectric skins discriminate static/dynamic pressure and temperature stimuli, Sci. Adv. 1 (2015), e1500661.
[17] Y. Chu, J. Zhong, H. Liu, Y. Ma, N. Liu, Y. Song, J. Liang, Z. Shao, Y. Sun, Y. Dong, X. Wang, L. Lin, Human pulse diagnosis for medical assessments using a wearable piezoelectret sensing system, Adv. Funct. Mater. 28 (2018), 1803413.
[18] C. Dagdeviren, Y. Su, P. Joe, R. Yona, Y. Liu, Y.S. Kim, Y. Huang, A.R. Damadoran, J. Xia, L.W. Martin, Y. Huang, J.A. Rogers, Conformable amplified lead zirconate titanate sensors with enhanced piezoelectric response for cutaneous pressure monitoring, Nat. Commun. 5 (2014) 4496.
[19] X. Han, X. Chen, X. Tang, Y.-L. Chen, J.-H. Liu, Q.-D. Shen, Flexible polymer transducers for dynamic recognizing physiological signals, Adv. Funct. Mater. 26 (2016) 3640–3648.
[20] C.L. Choong, M.B. Shim, B.S. Lee, S. Jeon, D.S. Ko, T.H. Kang, J. Bae, S.H. Lee, K. E. Byun, J. Im, Y.J. Jeong, C.E. Park, J.J. Park, U.I. Chung, Highly stretchable resistive pressure sensors using a conductive elastomeric composite on a micropyramid array, Adv. Mater. 26 (2014) 3451–3458.
[21] Y. Jin, G. Chen, K. Lao, S. Li, Y. Lu, Y. Gan, Z. Li, J. Hu, J. Huang, J. Wen, H. Deng, M. Yang, Z. Chen, X. Hu, B. Liang, J. Luo, Identifying human body states by using a flexible integrated sensor, npj Flex. Electron. 4 (2020) 28.
[22] C. Pang, G.Y. Lee, T.I. Kim, S.M. Kim, H.N. Kim, S.H. Ahn, K.Y. Suh, A flexible and highly sensitive strain-gauge sensor using reversible interlocking of nanofibres, Nat. Mater. 11 (2012) 795–801.
[23] T. Yang, W. Deng, X. Chu, X. Wang, Y. Hu, X. Fan, J. Song, Y. Gao, B. Zhang, G. Tian, D. Xiong, S. Zhong, L. Tang, Y. Hu, W. Yang, Hierarchically microstructure-bioinspired flexible piezoresistive bioelectronics, Acs Nano 15 (2021) 11555–11563.
[24] Z. He, W. Chen, B. Liang, C. Liu, L. Yang, D. Lu, Z. Mo, H. Zhu, Z. Tang, X. Gui, Capacitive pressure sensor with high sensitivity and fast response to dynamic interaction based on graphene and porous nylon networks, ACS Appl. Mater. Interfaces 10 (2018) 12816–12823.
[25] Q. Lin, J. Huang, J. Yang, Y. Huang, Y. Zhang, Y. Wang, J. Zhang, Y. Wang, L. Yuan, M. Cai, X. Hou, W. Zhang, Y. Zhou, S.G. Chen, C.F. Guo, Highly sensitive flexible iontronic pressure sensor for fingertip pulse monitoring, Adv. Health Mater. 9 (2020), e2001023.
[26] C. Pang, J.H. Koo, A. Nguyen, J.M. Caves, M.G. Kim, A. Chortos, K. Kim, P.J. Wang, J.B. Tok, Z. Bao, Highly skin-conformal microhairy sensor for pulse signal amplification, Adv. Mater. 27 (2015) 634–640.
[27] G. Schwartz, B.C. Tee, J. Mei, A.L. Appleton, D.H. Kim, H. Wang, Z. Bao, Flexible polymer transistors with high pressure sensitivity for application in electronic skin and health monitoring, Nat. Commun. 4 (2013) 1859.
[28] H. Ouyang, J. Tian, G. Sun, Y. Zou, Z. Liu, H. Li, L. Zhao, B. Shi, Y. Fan, Y. Fan, Z. L. Wang, Z. Li, Self-powered pulse sensor for antidiastole of cardiovascular disease, Adv. Mater. 29 (2017), 1703456.
[29] X. Wang, J. Yang, Z. Feng, G. Zhang, J. Qiu, Y. Wu, J. Yang, Graded microstructured flexible pressure sensors with high sensitivity and an ultrabroad pressure range for epidermal pulse monitoring, ACS Appl. Mater. Interfaces 13 (2021) 55747–55755.
[30] X. Wang, J. Yang, K. Meng, Q. He, G. Zhang, Z. Zhou, X. Tan, Z. Feng, C. Sun, J. Yang, Z.L. Wang, Enabling the unconstrained epidermal pulse wave monitoring via finger-touching, Adv. Funct. Mater. 31 (2021), 2102378.
[31] L. Xu, Z. Zhang, F. Gao, X. Zhao, X. Xun, Z. Kang, Q. Liao, Y. Zhang, Self-powered ultrasensitive pulse sensors for noninvasive multi-indicators cardiovascular monitoring, Nano Energy 81 (2021), 105614.
[32] J. Yang, J. Chen, Y. Su, Q. Jing, Z. Li, F. Yi, X. Wen, Z. Wang, Z.L. Wang, Eardrum-inspired active sensors for self-powered cardiovascular system characterization and throat-attached anti-interference voice recognition, Adv. Mater. 27 (2015) 1316–1326.
[33] S. Cho, Y. Yun, S. Jang, Y. Ra, J.H. Choi, H.J. Hwang, D. Choi, D. Choi, Universal biomechanical energy harvesting from joint movements using a direction-switchable triboelectric nanogenerator, Nano Energy 71 (2020), 104584.
[34] Z. Liu, L. Xu, Q. Zheng, Y. Kang, B. Shi, D. Jiang, H. Li, X. Qu, Y. Fan, Z.L. Wang, Z. Li, Human motion driven self-powered photodynamic system for long-term autonomous cancer therapy, ACS Nano 14 (2020) 8074–8083.
[35] Z. Liu, Q. Zheng, Y. Shi, L. Xu, Y. Zou, D. Jiang, B. Shi, X. Qu, H. Li, H. Ouyang, R. Liu, Y. Wu, Y. Fan, Z. Li, Flexible and stretchable dual mode nanogenerator for rehabilitation monitoring and information interaction, J. Mater. Chem. B 8 (2020) 3647–3654.
[36] C.L. Choong, M.B. Shim, B.S. Lee, S. Jeon, D.S. Ko, T.H. Kang, J. Bae, S.H. Lee, K. E. Byun, J. Im, Y.J. Jeong, C.E. Park, J.J. Park, U.I. Chung, Highly stretchable resistive pressure sensors using a conductive elastomeric composite on a micropyramid array, Adv. Mater. 26 (2014) 3451–3458.
[37] Z. Wang, L. Zhang, J. Liu, H. Jiang, C. Li, Flexible hemispheric microarrays of highly pressure-sensitive sensors based on breath Fig. method, Nanoscale 10 (2018) 10691–10698.
[38] J. Zhang, L.J. Zhou, H.M. Zhang, Z.X. Zhao, S.L. Dong, S. Wei, J. Zhao, Z.L. Wang, B. Guo, P.A. Hu, Highly sensitive flexible three-axis tactile sensors based on the interface contact resistance of microstructured graphene, Nanoscale 10 (2018) 7387–7395.
[39] B. Zhu, Z. Niu, H. Wang, W.R. Leow, H. Wang, Y. Li, L. Zheng, J. Wei, F. Huo, X. Chen, Microstructured graphene arrays for highly sensitive flexible tactile sensors, Small 10 (2014) 3625–3631.
[40] M.R. Nelson, J. Stepanek, M. Cevette, M. Covalciuc, R.T. Hurst, A.J. Tajik, Noninvasive measurement of central vascular pressures with arterial tonometry: clinical revival of the pulse pressure waveform? Mayo Clin. Proc. 85 (2010) 460–472.
[41] W. Fan, Q. He, K. Meng, X. Tan, Z. Zhou, G. Zhang, J. Yang, Z.L. Zhong, Machine-knitted washable sensor array textile for precise epidermal physiological signal monitoring, Sci. Adv. 6 (2020) eaay2840.

Xue Wang received her B.E. degree in school of measurement and communication engineering of Harbin University of Science and Technology. Now, she is a Ph.D. student in college of optoelectronic engineering, Chongqing University. Her current research is nanogenerator, self-powered sensor and systems.

Zhiping Feng received her B.E. degree in college of chemistry and materials science from Sichuan Normal University. Now, she is a Ph.D. student in college of optoelectronic engineering, Chongqing University. Her current research is self-powered sensor based on triboelectric nanogenerator and capacitive sensor.

Yushu Xia received her B.E. degree in School of Information Science and Engineering from Shenyang University of Technology. Now, she is an M.S. student in college of optoelectronic engineering, Chongqing University. Her current research is on flexible acoustic sensors based on triboelectric nanogenerator.

Gaoqiang Zhang is currently pursuing his Ph.D. degree in college of optoelectronic engineering, Chongqing University. He received his M.S degree from Qingdao University of Technology, China, in 2017. His research focuses upon Passive wireless sensor, multifunctional wearable electronics and low-power data acquisition and wireless monitoring system.

Luna Wang received her B.E. degree from the School of Mechanical Engineering, North China University of Water Resources and Electric Power. She is currently a M.S. student at the School of Optoelectronic Engineering, Chongqing University. Her current research is low frequency signal processing and machine learning modeling.

Liang Chen graduated from Sichuan University of Science & Engineering with a B.E. degree in mechanical engineering. Now, he is a M.S. student in the School of Optoelectronic Engineering, Chongqing University. His current research is on pulse-based identity recognition.

Dr. Yufen Wu received the B.E., M.E. and Ph.D. degrees in instrumentation science and technology from Chongqing University in 2005, 2008, and 2015, respectively. Currently, She is a teacher with the College of Physics and Electronic Engineering, Chongqing Normal University. Her current research interests focus on self-powered sensor and systems, measurement and instrumentation.

Dr. Jin Yang received the B.E., M.E. and Ph.D. degrees in instrumentation science and technology from Chongqing University in 2002, 2004, and 2007, respectively. Currently, he is a professor with the College of Optoelectronic Engineering, Chongqing University. His current research interests focus on sensor and actuator, measurement and instrumentation, nanogenerator, self-powered sensor and systems.

Zhong Lin Wang is the Hightower Chair in Materials Science and Engineering and Regents' Professor at Georgia Tech, and Founding Director and Chief Scientist at Beijing Institute of Nanoenergy and Nanosystems, Chinese Academy of Sciences. His discovery and breakthroughs in developing nanogenerators and self-powered nanosystems establish the principle and technological roadmap for harvesting mechanical energy from environmental and biological systems for powering personal electronics and future sensor networks. He coined and pioneered the field of piezotronics and piezophototronics.